Clin. Lab. 2025;71:XXX-XXX
©Copyright

ORIGINAL ARTICLE

Screening of Metabolism-Related Biomarkers and Construction of Prognostic Models in Patients with Neuroblastoma

Feng-Zhi Gu [1, *], Liang-Yu Mi [2, *], Bin Liu [3], Xian-Wu Yang [1], Ying-Quan Zhuo [1], Hua-Jian Gu [1]

[*] *Feng-Zhi Gu and Liang-Yu Mi contributed equally to this work*
[1] *Department of Pediatric Surgery, The Affiliated Hospital of Guizhou Medical University, Guiyang City, Guizhou Province, China*
[2] *Department of Rheumatology and Immunology, Third Hospital of Shanxi Medical University, Shanxi Bethune Hospital, Shanxi Academy of Medical Sciences, Tongji Shanxi Hospital, Taiyuan City, Shanxi Province, China*
[3] *Department of Endocrinology, Huai'an Hospital of Traditional Chinese Medicine, Huai'an City, Jiangsu Province, China*

SUMMARY

Background: **Energy metabolism (EM) genes play crucial roles in tumor development and progression. While neuroblastoma (NBL) cells exhibit high proliferation rates requiring efficient energy metabolism, the underlying mechanisms remain incompletely understood.**
Methods: **Transcriptomic analysis of the TARGET-NBL dataset was performed to stratify samples based on EM-related gene expression. Differential expression analysis and weighted gene co-expression network analysis (WGCNA) were integrated to identify critical gene modules. Prognostic biomarkers were determined through univariate and multivariate Cox regression analyses. Functional enrichment analysis and drug prediction were conducted for the identified biomarkers. Expression levels of candidate genes (GRIA2, FBXO32, GNG12, and PHLDA2) were validated using qRT-PCR. The biological function of GNG12 was investigated through gain- and loss-of-function studies in neuroblastoma cell lines.**
Results: **The analysis identified 1,675 differentially expressed genes and two critical modules (MEblack and MEturquoise) through WGCNA. Four prognostic biomarkers (GRIA2, FBXO32, GNG12, and PHLDA2) were established and integrated into a nomogram with clinical parameters. Functional analysis revealed their involvement in extracellular matrix organization, DNA replication, and nucleocytoplasmic transport. Drug prediction identified potential therapeutic compounds targeting GRIA2 and FBXO32. Experimental validation demonstrated elevated expression of all four biomarkers in neuroblastoma cell lines compared to normal controls. Notably, GNG12 knockdown significantly suppressed while its overexpression enhanced proliferation and migration of SH-SY5Y cells.**
Conclusions: **This study identified and validated four EM-related prognostic biomarkers in neuroblastoma, with GNG12 functionally implicated in tumor cell proliferation and migration. These findings provide potential therapeutic targets and prognostic indicators for neuroblastoma management.**
(Clin. Lab. 2025;71:xx-xx. DOI: 10.7754/Clin.Lab.2025.250323)

Correspondence:
Hua-Jian Gu
Department of Pediatric Surgery
The Affiliated Hospital of Guizhou Medical University
No. 28 Guiyi Street
Guiyang City, 550004
Guizhou Province
China
Email: Guhuajian_gululu@hotmail.com

Manuscript accepted April 3, 2025

KEYWORDS

energy metabolism, neuroblastoma, prognosis, biomarkers, GNG12

INTRODUCTION

Neuroblastoma (NB), an embryonal tumor of the sympathetic nervous system, is the most common extracranial solid malignancy in childhood, comprising 7% of

pediatric cancers and contributing to 15% of cancer-related deaths in children [1]. Based on the International Neuroblastoma Risk Group (INRG) classification system, NB stratification encompasses three distinct risk categories (low, intermediate, and high), incorporating multiple clinicopathological parameters including age at initial diagnosis, INSS staging, DNA ploidy index, MYCN amplification status, and histopathological differentiation, thereby facilitating risk-adapted therapeutic interventions [2]. The current therapeutic armamentarium for neuroblastoma encompasses multimodal interventions, including surgical resection, systemic chemotherapy, external beam radiation therapy, autologous hematopoietic stem cell transplantation (HSCT), and immunotherapeutic approaches [3]. While survival rates for NB have significantly improved in recent decades, particularly in the low-risk group where overall survival rates surpass 90% [4], the high-risk group still faces challenges with cure rates remaining below 30% despite comprehensive treatments [5], and adverse effects such as cognitive dysfunction and drug resistance associated with radiotherapy and chemotherapy. Therefore, elucidating the metabolic phenotypes and underlying molecular regulatory networks of neuroblastoma is imperative for the identification of novel therapeutic targets and the development of more efficacious interventions, ultimately contributing to improved clinical outcomes and long-term survival in neuroblastoma patients.

Energy metabolism is one of the fundamental features of life, wherein organisms acquire nutrients from the environment, metabolize them internally to release stored chemical energy, and utilize it to sustain life processes, involving energy release, transfer, storage, and utilization. Metabolic reprogramming, a fundamental hallmark of malignant transformation, facilitates cellular bioenergetics through enhanced adenosine triphosphate (ATP) generation, while maintaining redox homeostasis and supporting macromolecular biosynthesis essential for neoplastic proliferation, survival, and metastatic potential. Accumulating evidence has demonstrated that genes regulating cellular energetics play pivotal roles in the initiation, progression, and metastatic dissemination of diverse malignancies [6]. Neuroblastoma cells exhibit an accelerated proliferative rate, necessitating robust metabolic adaptation and optimized energy utilization. In neuroblastoma, cells may rely on enhanced glycolysis processes (i.e. the "Warburg effect"), prioritizing glycolysis for energy production even under adequate oxygen supply. In response to dynamic alterations in tumor microenvironment, neuroblastoma-derived exosomes harbor diverse metabolic enzymes that orchestrate key bioenergetic pathways, including glycolysis, tricarboxylic acid (TCA) cycle, oxidative phosphorylation, fatty acid β-oxidation, malate-aspartate shuttle system, and glutamine catabolism, establishing an intricate metabolic network essential for tumor adaptation. Cancer cells typically undergo metabolic reprogramming, altering the way energy is metabolized to meet the demands of rapid cell growth and division [7].

This study aimed to systematically identify and validate energy metabolism-associated prognostic biomarkers in neuroblastoma through integrated bioinformatic approaches, incorporating differential expression analysis, weighted gene co-expression network analysis (WGC NA), and Cox proportional hazards modeling. Furthermore, this investigation sought to elucidate the functional implications of these metabolic signatures and establish a robust prognostic stratification system, ultimately providing novel therapeutic perspectives for precision medicine in neuroblastoma management.

MATERIALS AND METHODS

Data sources

Clinical and molecular data were retrieved from the Therapeutically Applicable Research to Generate Effective Treatments (TARGET) database (https://ocg.cancer.gov/programs/target/), specifically the TARGET -NBL cohort, comprising 158 neuroblastoma cases with comprehensive clinicopathological annotations. Moreover, the E-MTAB-8248 dataset including 223 NBL samples with the corresponding clinical information were acquired from the Array Express online database (https://www.ebi.ac.uk/arrayexpress/experiments/E-MTAB-8248/) for the verification of risk model. Furthermore, pathways related to human metabolism were obtained through the Reactome online database (https://reactome.org/). The energy metabolism (EM) related-genes were achieved from 11 metabolic pathways.

The differential expression analysis and enrichment analysis

Expression profiles of energy metabolism-related genes in the TARGET-NBL dataset were analyzed using gene set variation analysis (GSVA, v1.46.0) to generate sample-specific enrichment scores, facilitating stratification into high- and low-score cohorts. Survival disparities between these subgroups were evaluated through Kaplan-Meier analysis with log-rank test. Differential expression analysis was performed using DESeq2 (v1.36.0), with significantly differentially expressed genes (DEGs) identified based on stringent criteria (adjusted p-value < 0.05 and $|\log2FoldChange| > 1$). The transcriptional landscape was visualized through hierarchical clustering heatmaps and volcano plots using pheatmap (v1.0.12) and ggplot2 (v3.3.5) packages, respectively. Functional characterization of the DEGs was conducted through Gene Ontology (GO) and Kyoto Encyclopedia of Genes and Genomes (KEGG) pathway enrichment analyses utilizing clusterProfiler (v3.8.1), with significant enrichment defined as adjusted p-value < 0.05.

The WGCNA and screening of overlapping genes

Weighted gene co-expression network analysis (WGC NA) was implemented across the TARGET-NBL cohort to identify biologically relevant modules. Initially, hierarchical clustering was performed for quality control, facilitating the removal of outlier samples to enhance analytical robustness. An optimal soft-thresholding power (β) was determined to establish scale-free topology, followed by module identification through dynamic tree-cutting algorithm. Module-trait associations were evaluated by correlating module eigengenes with the GSVA enrichment scores of energy metabolism-related genes. Modules exhibiting maximal positive and negative correlation coefficients with the metabolic signature were designated as critical modules. Subsequently, intersection analysis between differentially expressed genes (DEGs) and genes within the critical modules was conducted to identify core regulatory elements.

Verification and construction of risk model

Prognostic significance of the identified overlapping genes was initially evaluated through univariate Cox proportional hazards regression analysis and proportional hazards assumption testing ($p < 0.05$). Subsequently, multivariate Cox regression analysis with stepwise feature selection was implemented to identify robust prognostic biomarkers. A risk stratification model was constructed based on the expression profiles of these identified biomarkers, with the risk score calculated as (risk score = $\sum_1^n \mathrm{coef}(\mathrm{gene_i}) * expression(\mathrm{gene_i})$). Patient stratification into high- and low-risk subgroups was performed using the median risk score as the dichotomization threshold in both the TARGET-NBL discovery cohort and the E-MTAB-8248 validation cohort. The prognostic performance of the risk model was assessed through Kaplan-Meier survival analysis with log-rank test and time-dependent receiver operating characteristic (ROC) curve analysis at 1-, 3-, and 5-year intervals.

Clinical correlation analysis

The distribution of clinical features including MYCN amplification, age, INSS staging, MKI, and grade between high- and low-score groups were analyzed. Besides, the survival analyses of those five different clinical features were further analyzed between the two risk subgroups.

Independent prognostic analysis

Independent prognostic value assessment was conducted through univariate and multivariate Cox regression analyses, incorporating both established clinicopathological parameters (mitosis-karyorrhexis index [MKI], age at diagnosis, and other relevant variables) and the derived risk score. Variables demonstrating statistical significance in univariate analysis were subsequently integrated into multivariate Cox proportional hazards modeling to identify independent prognostic factors. A comprehensive prognostic nomogram was constructed integrating these independent factors to predict 1-, 3-, and 5-year overall survival probabilities for neuroblastoma patients. The predictive accuracy and discriminative ability of the nomogram were evaluated through calibration curve analysis comparing predicted versus observed survival probabilities.

Enrichment analysis

To elucidate the underlying molecular mechanisms and functional pathways associated with the identified biomarkers, gene set enrichment analysis (GSEA) was performed utilizing the clusterProfiler package (v3.8.1), with significance threshold set at adjusted p-value < 0.05 for pathway enrichment.

Chemosensitivity analysis and drug prediction

Therapeutic response prediction was performed utilizing pharmacogenomic data from the Genomics of Drug Sensitivity in Cancer (GDSC) database (https://www.cancerrxgene.org/), encompassing 198 chemotherapeutic agents. The half-maximal inhibitory concentration (IC_{50}) values were computationally predicted through integration of GDSC cell line expression profiles and neuroblastoma transcriptomic data. Differential drug sensitivity analysis between risk-stratified subgroups was conducted using the Wilcoxon rank-sum test. Additionally, potential therapeutic agents targeting the identified biomarkers were systematically explored through comprehensive mining of the DrugBank database (https://go.drugbank.com/) and the Drug-Gene Interaction Database (DGIdb, www.dgidb.org). Subsequently, a biomarker-drug interaction network was constructed to visualize potential therapeutic interventions.

Cell lines and cell culture

Three neuroblastoma cell lines (SK-N-SH, SH-SY5Y, and IMR-32) were maintained in their respective culture media: Dulbecco's Modified Eagle Medium (DMEM) supplemented with 10% fetal bovine serum (FBS) for SK-N-SH; Modified Eagle Medium/Nutrient Mixture F-12 (MEM/F12) with 10% FBS for SH-SY5Y; and Modified Eagle Medium (MEM) containing 10% FBS for IMR-32. Non-malignant control cell lines included human lung fibroblasts (MRC-5), cultured in high-glucose DMEM supplemented with 10% FBS and 1% penicillin/streptomycin (P/S), and human embryonic kidney cells (HEK293), maintained in MEM supplemented with 10% FBS. All cell lines were obtained from Nanjing Kaiji Biologicals Corporation (Nanjing, China) and maintained at 37°C in a humidified atmosphere containing 5% CO_2.

qRT-PCR for gene expression detection

Total RNA extraction was performed using TRIzol® reagent (Invitrogen, Cat. no. 15596-026, USA) according to the manufacturer's protocol. First-strand cDNA synthesis was conducted using the PrimeScript™ RT Reagent Kit (TaKaRa, Cat. no. RR036B, Japan). Quantitative real-time PCR (qRT-PCR) was performed using TB Green® Premix Ex Taq™ II (Tli RNaseH Plus) (TaKa-

Ra, Cat. no. RR820A, Japan) on a thermal cycler. Glyceraldehyde 3-phosphate dehydrogenase (GAPDH) served as the endogenous normalization control. Relative gene expression levels were quantified using the comparative threshold cycle method ($2^{-\Delta\Delta Ct}$). Sequence-specific primers utilized in this study are detailed in Table 1.

Oligo or vector transfection

Both the small interfering RNA (siRNA) to knock down GNG12 to GNG12 and the construction of the GNG12 overexpression pcDNA vector (GNG12-oe) were provided by Jiangsu KGI Biological Co. Oligo or vector was transfected into SH-SY5Y cells using Lipofectamine 3000 reagent (Invitrogen, USA).

CCK-8 assay for cell proliferation detection

The experimental cells were inoculated into 96-well plates (5,000 cells/well). The cells were then cultured in an incubator until they adhered to the wall. After 24 hours of incubation, the OD values were determined at 24, 48 and 72 hours. Prior to each assay, CCK-8 reagent (Jiangsu Kaiji Biological Co., Ltd., China) was pipetted into each well and incubated for another 2 hours. The absorbance at 450 nm in each well was then detected using an enzyme-labelled spectrophotometer (TECAN SPARK, Switzerland).

Transwell assay for cell migration

Cell migration was evaluated using Transwell chambers. Cells were seeded in the upper chamber in serum-free medium, while complete medium containing 10% FBS was added to the lower chamber as a chemoattractant. Following 24-hour incubation at 37°C in 5% CO_2, non-migrated cells on the upper surface of the membrane were gently removed using cotton swabs. The migrated cells on the lower surface were fixed with 4% paraformaldehyde and stained with 0.1% crystal violet for 30 minutes at 37°C. After PBS washing, migrated cells were visualized under a light microscope. Images were captured from three random fields along the diameter at 200 × magnification, and quantification was performed using ImageJ software.

Statistical analyses

All analyses in this study were performed in R package, and the NBL datasets were acquired from the public database. Statistics were analyzed using GraphPad Prism software 10, and p-values were calculated using one-way ANOVA when significance tests were performed. $p < 0.05$ was considered a statistically significant difference.

RESULTS

Acquisition and enrichment analysis of DEGs

Kaplan-Meier analysis revealed significant survival differences between the two score-stratified subgroups ($p < 0.05$), with superior overall survival observed in the low-score cohort (Supplementary Figure 1). Differential expression analysis of the TARGET-NBL dataset identified 1,675 significantly differentially expressed genes (DEGs) between the score-stratified subgroups (Figure 1A, Supplementary Table 1). The transcriptional profiles of these DEGs were visualized through hierarchical clustering heatmap analysis (Figure 1B). Gene Ontology (GO) and Kyoto Encyclopedia of Genes and Genomes (KEGG) pathway enrichment analyses revealed significant enrichment of DEGs in biological processes including 'collagen-containing extracellular matrix', 'receptor ligand activity', and 'extracellular matrix organization', as well as signaling pathways such as 'Neuroactive Ligand-receptor interaction' and 'Complement and coagulation cascades' (Supplementary Figure 2A - B, Supplementary Tables 2 and3).

Acquisition of critical module and overlapping genes

Hierarchical clustering analysis demonstrated optimal sample quality with no outliers detected (Supplementary Figure 3A). A soft-thresholding power (β) of 12 was selected to achieve maximal scale-free topology fit (Supplementary Figure 3B). Module identification and dynamic tree cutting resulted in eight distinct co-expression modules after merging similar modules (Figure 2A). Correlation analysis of module-trait relationships identified two critical modules: the MEblack module (correlation coefficient = 0.51, p = 3e-11) comprising 1,729 genes, and the MEturquoise module (correlation coefficient = -0.64, p = 9e-19) containing 4,305 genes (Figure 2B). Intersection analysis between differentially expressed genes and genes within these critical modules yielded 553 overlapping candidates (Figure 2C).

Four biomarkers were screened out

Univariate Cox regression analysis identified 15 prognostically significant candidates, including FMO3 and OGN (Supplementary Figure 4A). Subsequent multivariate Cox regression analysis refined these candidates to four independent prognostic biomarkers: GRIA2, FBXO32, GNG12, and PHLDA2 (Supplementary Figure 4B). Risk stratification of neuroblastoma patients in the TARGET-NBL cohort revealed a positive correlation between risk scores and mortality rates (Supplementary Figure 5A). Kaplan-Meier analysis demonstrated significantly superior overall survival in the low-risk group compared to the high-risk group ($p < 0.0001$) (Supplementary Figure 5B). The prognostic model exhibited robust predictive performance, with area under the receiver operating characteristic curve (AUC) values exceeding 0.7 for 1-, 3-, and 5-year survival predictions (Supplementary Figure 5C). External validation using the independent E-MTAB-8248 cohort corroborated these

Table 1. Sequences of PCR primers used for gene expression analysis.

Gene	Forward (5′ - 3′)	Reverse (5′ - 3′)
GNG12	GCACCAACAATATAGCCCAGG	TCACTCCTGGCATGTTCCTC
GRIA2	TGGCTACTGGAGTGAAGTGG	AGGTCAACACAGTAGCCCTC
FBX032	TGTGGGTGTATCGGATGGAG	AAAGGCAGGTCAGTGAAGGT
PHLDA2	CGCTTCCACTCCATCCTCAA	GGCGGTTCTGGAAATCGATG
GAPDH	CAAATTCCATGGCACCGTCA	AGCATCGCCCCACTTGATTT

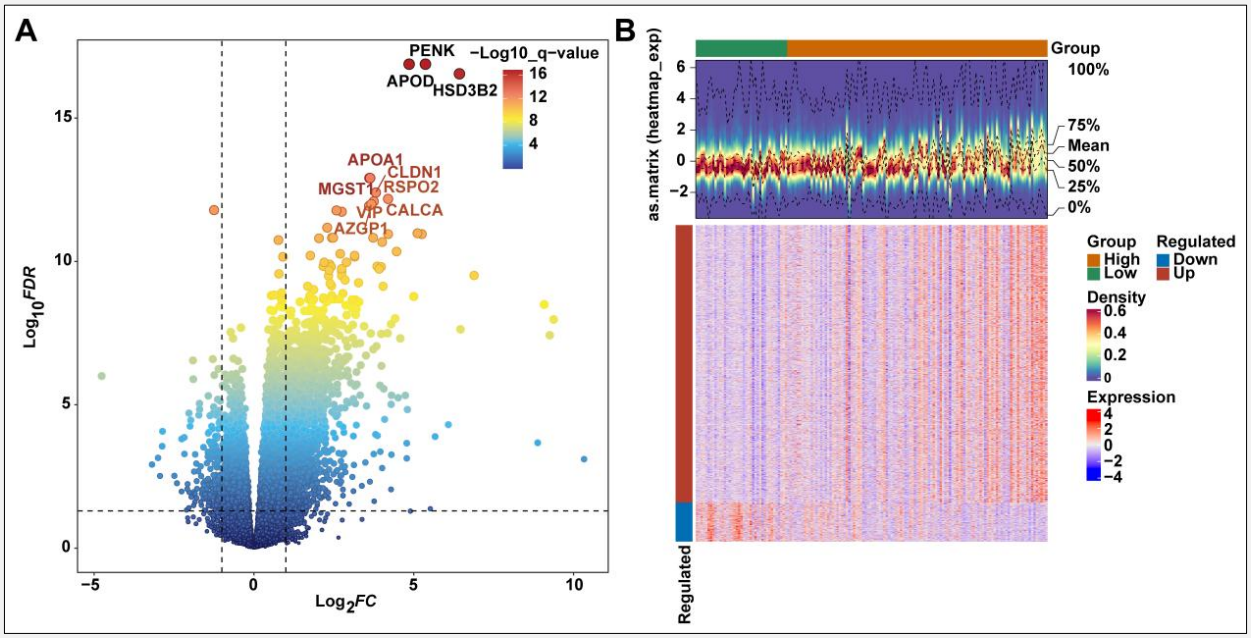

Figure 1. Acquisition of DEGs.

A - In the TARGET-NBL dataset, 1,675 DEGs were identified between the two score subgroups. B - Expression heat map of DEGs.

findings, demonstrating consistent prognostic stratification capability (Supplementary Figure 6A - C).

The clinical correlation analysis between two risk subgroups

When examining clinical features like age (≥ 1.5), INSS (stage 4), MKI (high and intermediate), and MYCN (amplified), the high-risk group of NBL patients outnumbered the low-risk group (Figure 3A - D, Supplementary Figure 7). Differences in survival were evident between the two groups concerning five clinical features, including age (≥ 1.5 and < 1.5), MYCN (not amplified), MKI (intermediate), INSS (stage 4), and grade (undifferentiated or poorly differentiated) (Supplementary Figures 8 - 10).

A nomogram was created

Univariate Cox regression analysis identified three significant prognostic variables ($p < 0.05$): risk score, age at diagnosis, and mitosis-karyorrhexis index (MKI) (Supplementary Figure 11A). These independent prognostic factors were subsequently integrated through multivariate Cox regression modeling (Supplementary Figure 11B). A comprehensive prognostic nomogram incorporating age at diagnosis, risk score, and MKI was constructed to predict 1-, 3-, and 5-year overall survival probabilities in neuroblastoma patients (Supplementary Figure 12A). The calibration plots demonstrated excellent concordance between nomogram-predicted and observed survival probabilities, validating the model's predictive accuracy (Supplementary Figure 12B).

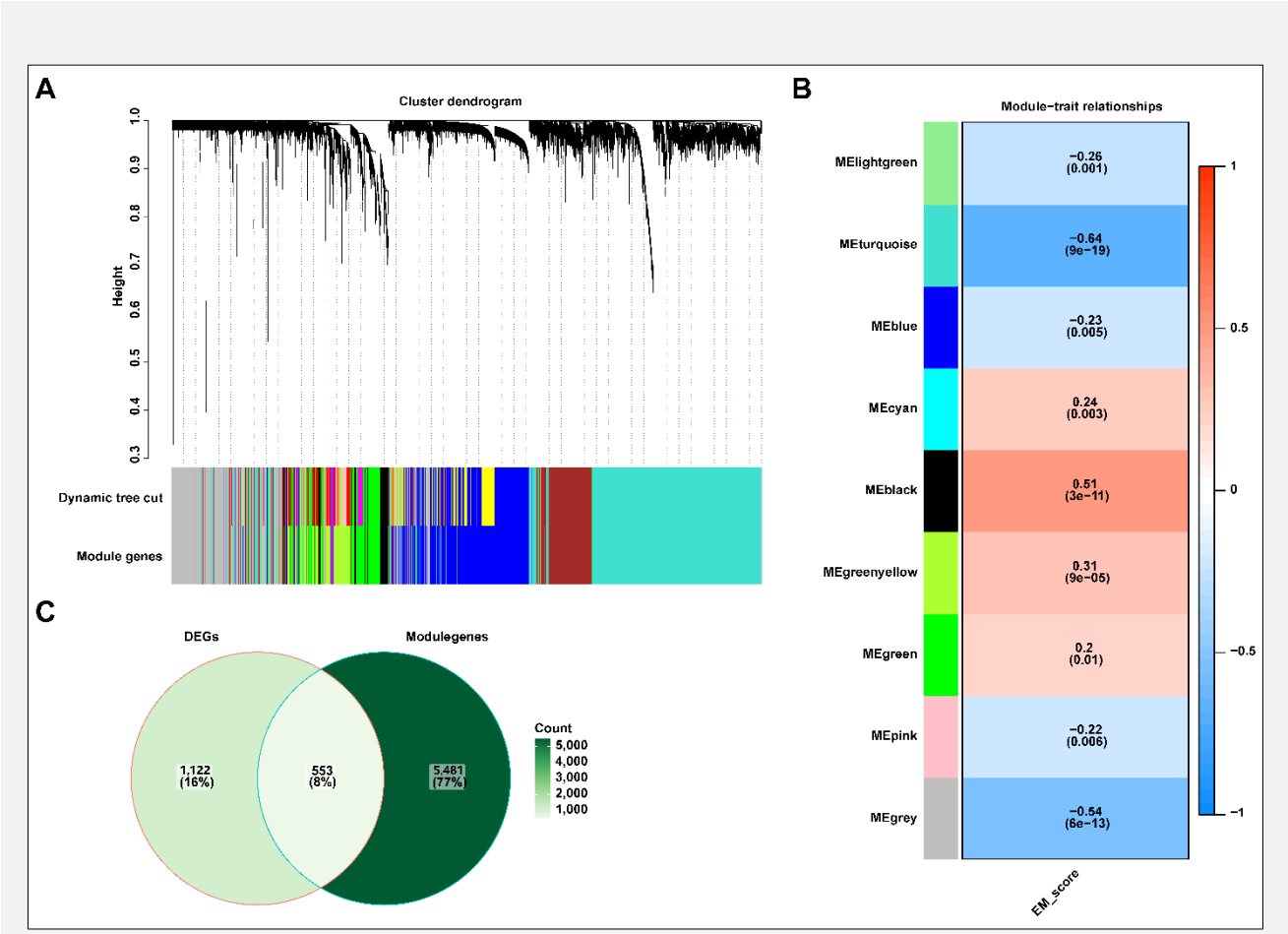

Figure 2. Acquisition of critical modules and overlapping genes.

A - Identification of eight gene modules after merging similar modules. B - Critical modules identified: MEblack containing 1,729 genes and MEturquoise containing 4,305 genes. C - A total of 553 overlapping genes were identified at the intersection of the critical modules.

The GSEA of the biomarkers

Gene set enrichment analysis (GSEA) elucidated the functional implications of the identified biomarkers. Gene Ontology (GO) analysis revealed that FBXO32 and GNG12 were significantly enriched in biological processes including 'Collagen-Containing Extracellular Matrix', 'DNA-Templated DNA Replication', and 'Chromosomal Region', while GRIA2 and PHLDA2 showed predominant enrichment in molecular functions such as 'Extracellular Matrix Structural Constituent'. Kyoto Encyclopedia of Genes and Genomes (KEGG) pathway analysis demonstrated that FBXO32 and GNG12 were primarily associated with 'DNA Replication' and 'Nucleocytoplasmic Transport' pathways, whereas GRIA2 and PHLDA2 exhibited significant enrichment in 'Viral Protein Interaction with Cytokine and Cytokine Receptor' signaling cascades (Supplementary Figures 13 - 16, Supplementary Tables 4 - 11).

Chemosensitivity analysis between two risk subgroups and drug prediction of biomarkers

There were 73 drugs with significant differences in IC_{50} between two risk subgroups, drugs with $p < 0.001$ and an average IC_{50} of less than 2 were displayed, such as Docetaxel, AZD7762, and so on (Figure 4, Supplementary Table 12). In addition, GRIA2 forecasted 28 drugs, and 5 drugs were predicted based on FBXO32 including Indoleacetic acid, PENTOBARBITAL, and so on (Figure 5).

Verification of gene expression levels by qRT-PCR

Expression profiles of the four identified biomarkers (GRIA2, FBXO32, GNG12, and PHLDA2) were validated using quantitative real-time PCR (qRT-PCR). Differential expression analysis revealed significant expression of all four genes across neuroblastoma cell lines (SK-N-SH, SH-SY5Y, and IMR-32). SK-N-SH

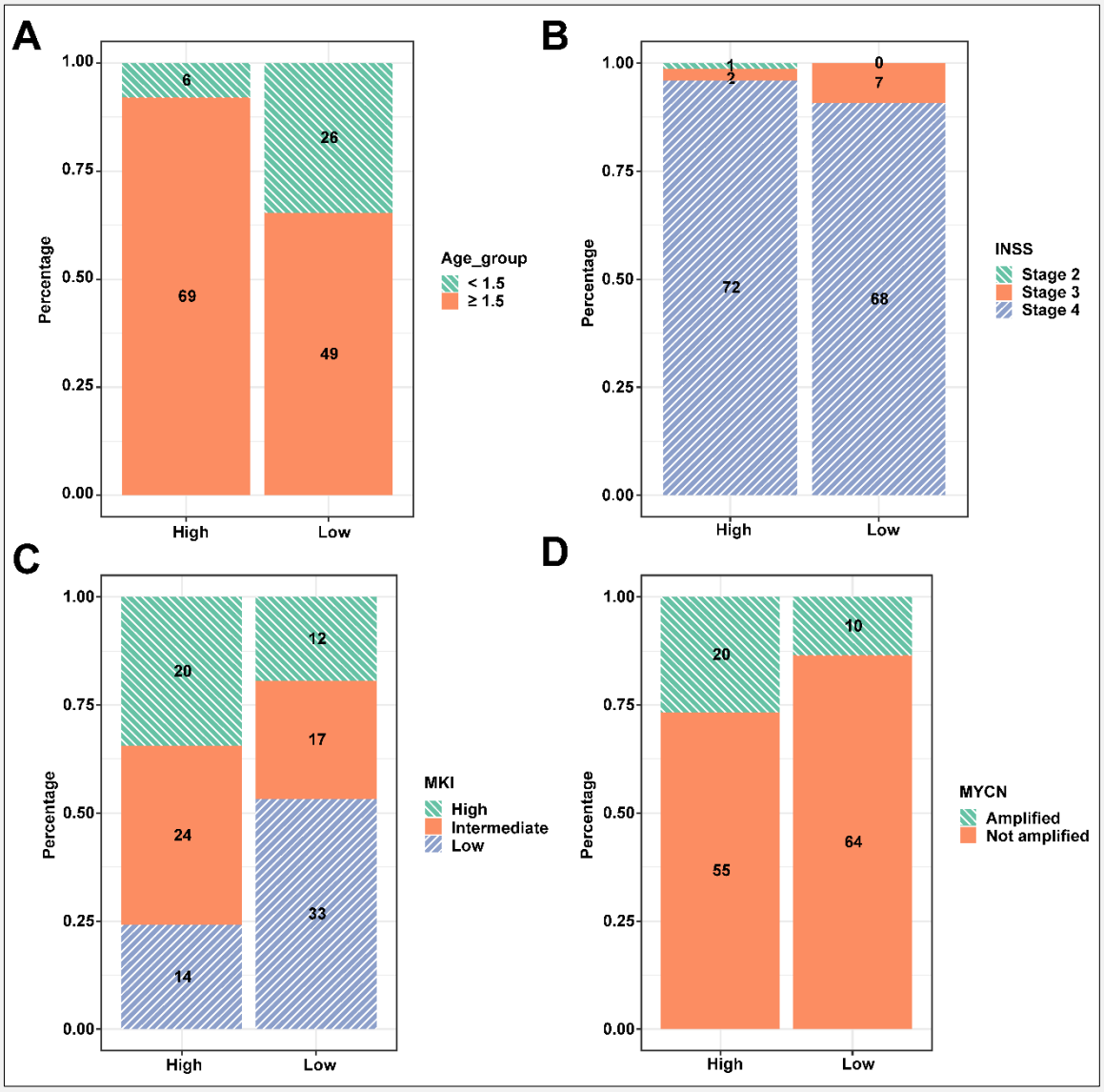

Figure 3. The clinical correlation analysis between two risk subgroups.

A - D - Higher distribution of clinical features including age (≥ 1.5), INSS (stage 4), MKI (high and intermediate), and MYCN (amplified) in the high-risk group.

demonstrated the highest expression levels among neuroblastoma lines, while GRIA2 exhibited significantly higher expression in IMR-32 compared to SH-SY5Y. FBXO32, GNG12, and PHLDA2 showed comparable expression levels between SH-SY5Y and IMR-32 cell lines (Figure 6A). Notably, all four biomarkers demonstrated significantly elevated expression in SH-SY5Y cells compared to non-malignant controls, including human lung fibroblasts (MRC-5) and human embryonic kidney cells (HEK293) (Figure 6B).

Effect of GNG12 on the proliferation and migration of neuroblastoma

For functional validation, GNG12 was selected as a candidate gene, and SH-SY5Y cells were chosen as an *in vitro* model system. Loss- and gain-of-function studies were performed using GNG12-specific small interfering RNA (siRNA) and overexpression vectors, respectively. qRT-PCR analysis confirmed successful manipulation of GNG12 expression, with significant downregulation observed in the knockdown group com-

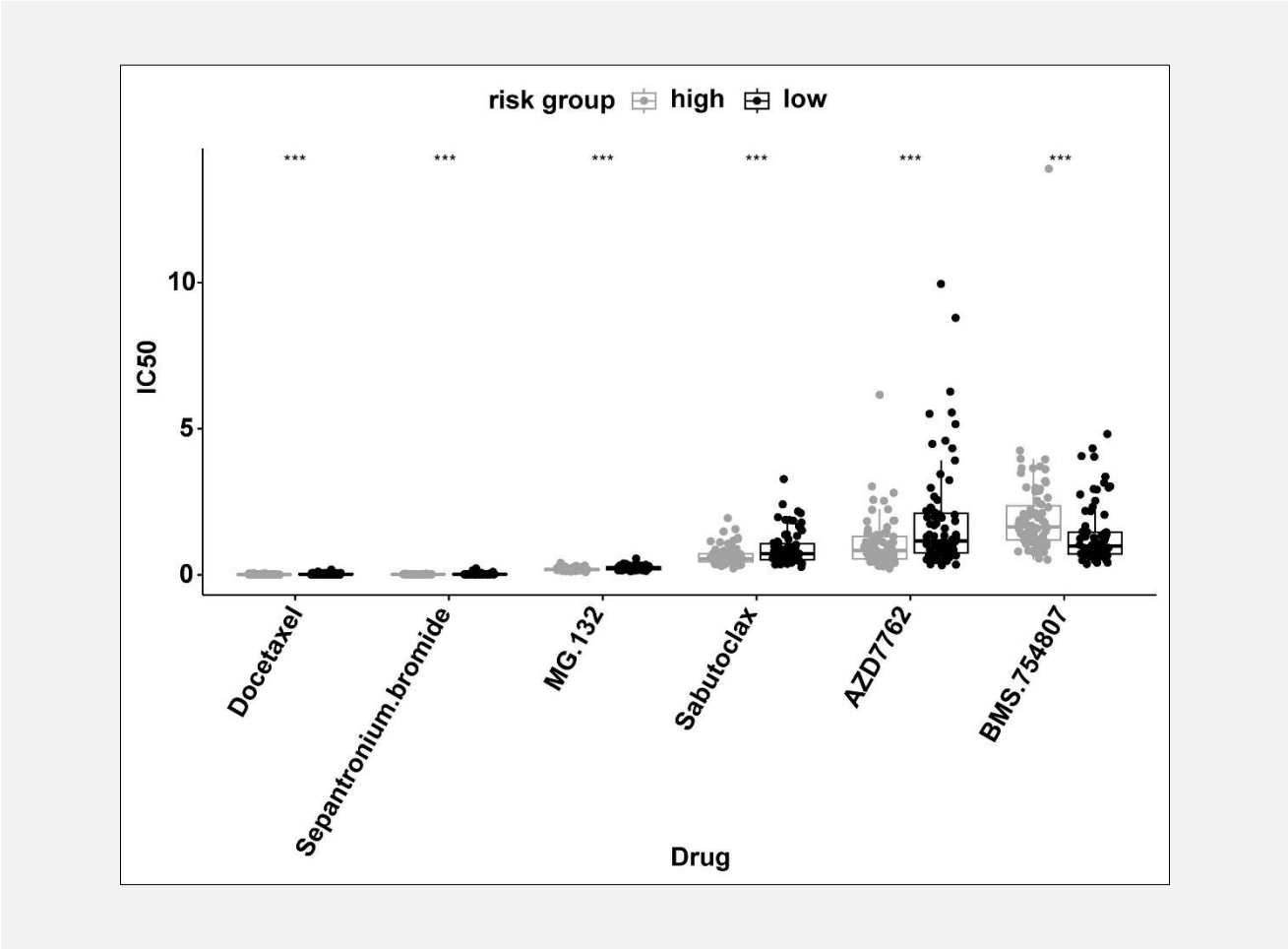

Figure 4. Chemosensitivity analysis between two risk subgroups.

pared to si-NC controls, and significant upregulation in the overexpression group relative to oe-NC controls (Figure 7A). Functional characterization of GNG12 was performed using cell viability and migration assays. Cell Counting Kit-8 (CCK-8) analysis demonstrated that GNG12 knockdown significantly suppressed proliferation of SH-SY5Y cells compared to negative controls, while GNG12 overexpression markedly enhanced cellular proliferation (Figure 7B). Consistent with these findings, Transwell migration assays revealed that GNG12 silencing significantly attenuated the migratory capacity of SH-SY5Y cells, whereas GNG12 overexpression substantially promoted cell migration (Figure 7C - D). These functional studies establish that GNG12 serves as a critical regulator of neuroblastoma cell proliferation and migration. The inverse correlation between GNG12 expression and cellular aggressive behavior suggests its potential role as a molecular driver in neuroblastoma progression. Furthermore, these findings provide mechanistic insights into the association between elevated GNG12 expression and poor clinical outcomes in neuroblastoma patients.

DISCUSSION

The study identified four biomarkers associated with NB: GRIA2, FBXO32, GNG12, and PHLDA2, which are involved in the pathogenesis of NB. GRIA2 encodes the GluR2/GluA2 subunit of the α-amino-3-hydroxy-5-methyl-4-isoxazolepropionic acid (AMPA)-type glutamate receptor, which plays a crucial role in regulating calcium ion permeability across neuronal membranes through its selective ion channel properties. Decreased calcium permeability upon glutamate receptor 2 insertion is integral to cellular calcium homeostasis and can influence synaptic plasticity or neurodegeneration [8]. Although GRIA2 exhibits predominant physiological expression in neural tissues, its aberrant expression has been documented in various neoplastic contexts, where it functions as a potential mediator of cellular proliferation, apoptosis, and invasion [9-11]. In vascular smooth muscle cells, GRIA2 has been shown to regulate proliferation and migration, potentially affecting restenosis post-percutaneous transluminal angioplasty (PTA) for peripheral arterial disease (PAD) [12]. Mutations in

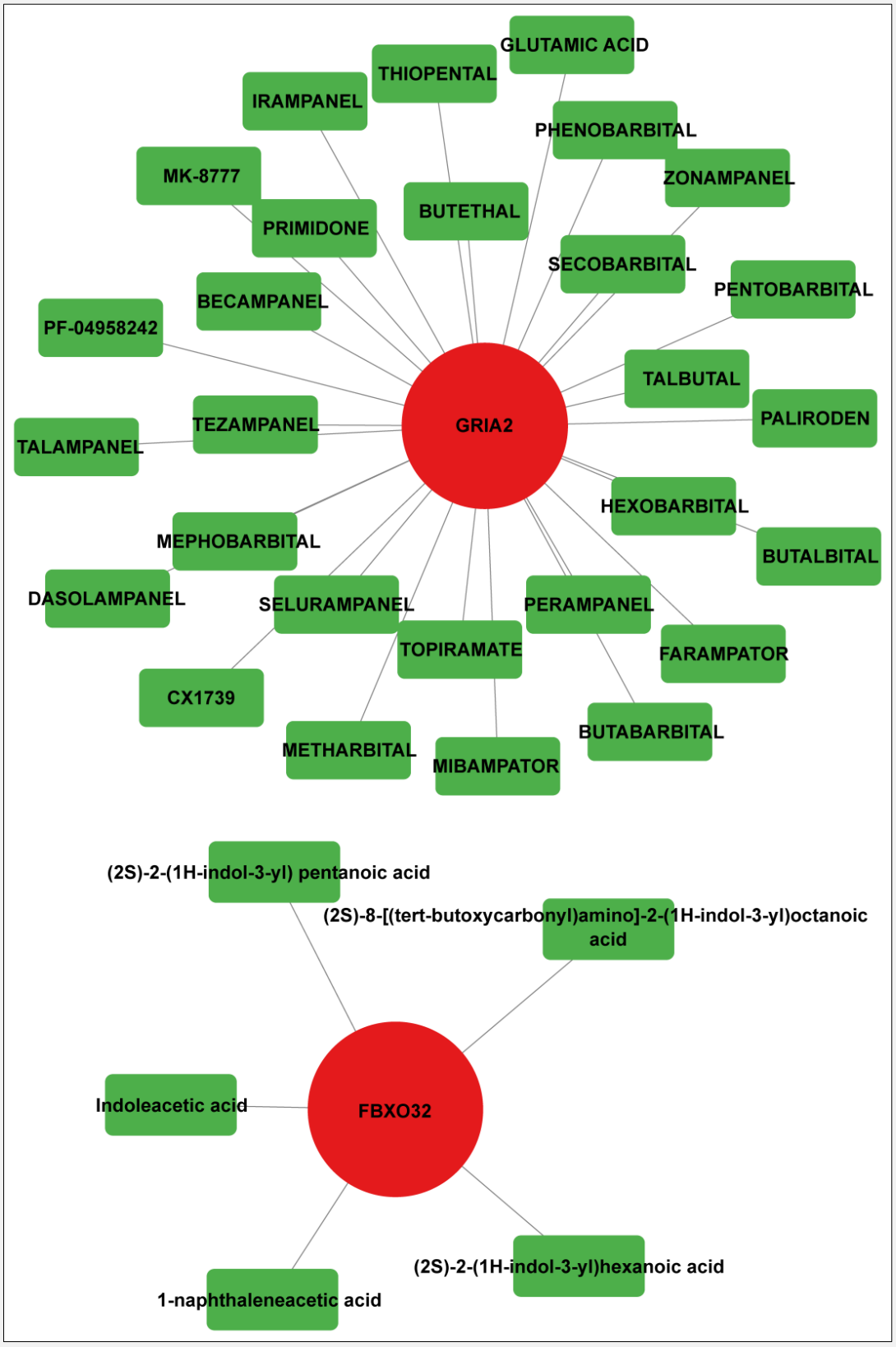

Figure 5. Prognostic genes' potential drug networks.

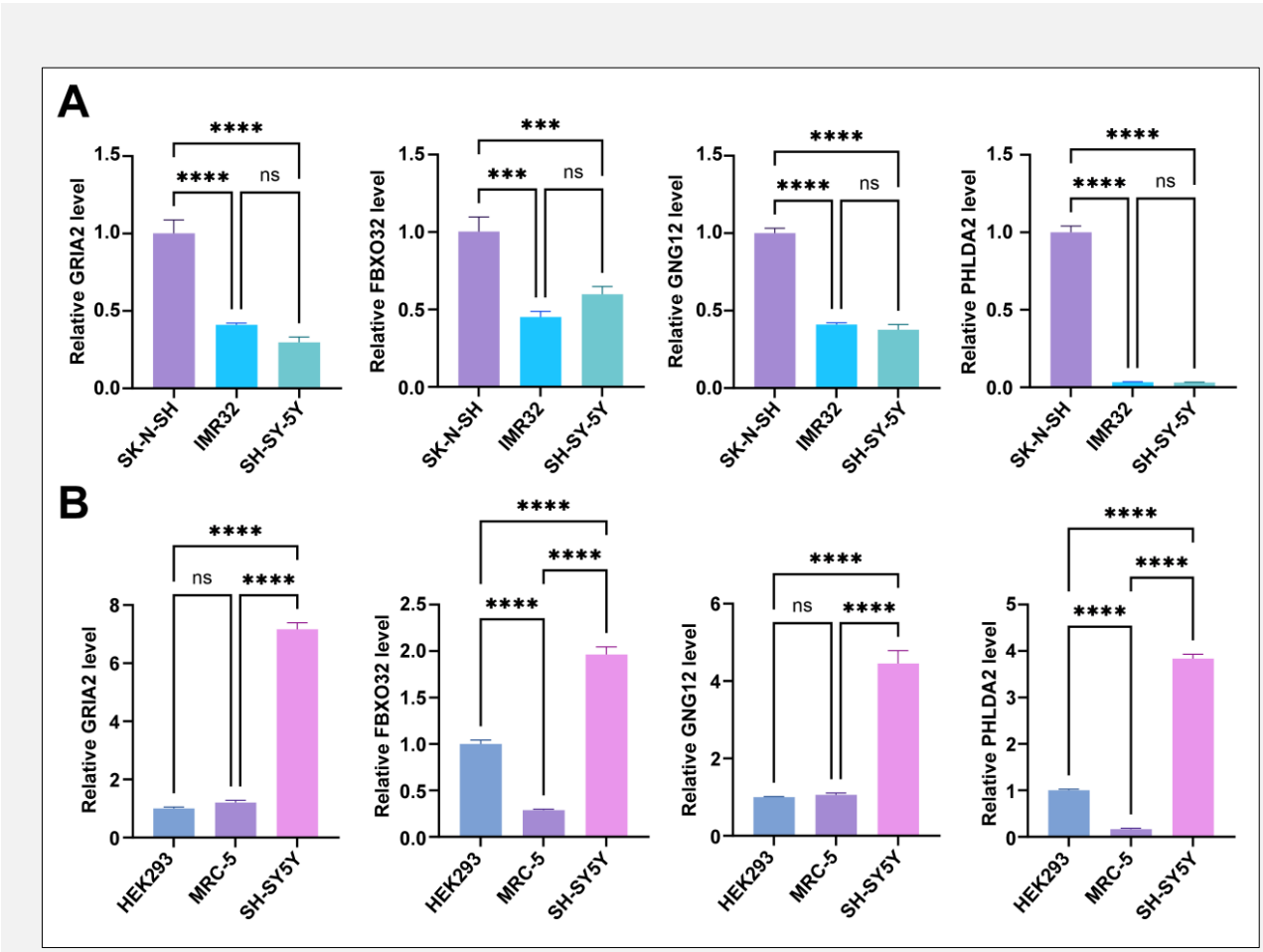

Figure 6. QRT-PCR experiments were performed to verify the expression levels of the four key genes in five cell lines.

A - QRT-PCR to detect the expression of four genes in neuroblastoma cell lines (SK-N-SH, SH-SY5Y, and IMR-32), B - QRT-PCR to detect the expression of four genes in neuroblastoma cell lines SH-SY5Y, MRC-5, and HEK293 (** - $p < 0.0001$, *** - $p < 0.001$, ** - $p < 0.01$, * - $p < 0.05$).**

GRIA2 that disrupt AMPAR function are associated with epilepsy, intellectual disabilities, and various neurodevelopmental disorders [13]. Transcriptomic profiling has established GRIA2 as a molecular diagnostic biomarker for solitary fibrous tumors (SFTs), facilitating differential diagnosis in soft tissue neoplasms [14]. These observations collectively underscore the multifaceted role of GRIA2 in various cancers and physiological processes, highlighting its potential as biomarker and therapeutic target.

FBXO32 (F-box protein 32), alternatively designated as Atrogin-1/MAFbx, belongs to the F-box protein family and functions as a substrate-recognition component of the SKP1-CUL1-F-box (SCF) E3 ubiquitin ligase complex, which orchestrates protein ubiquitination and subsequent proteasomal degradation. Accumulating evidence has established FBXO32 as a tumor suppressor [15,16]. Moreover, in gliomas, chemoresistance to temozolomide is associated with downregulation of BASP1. BASP1 loss leads to upregulation of FBXO32 in non-methylated and methylated gliomas. Increased H3K4me3 and H3K9ac at the FBXO32 promoter region enhance activation of the NF-κB/MGMT axis [17]. In neuroblastoma pathogenesis, FBXO32 functions as a critical post-translational regulator through its E3 ubiquitin ligase activity, orchestrating cellular proliferation, cell cycle dynamics, and survival signaling via selective protein degradation of key pathway components.

Pleckstrin homology-like domain family A member 2 (PHLDA2), positioned within the tumor suppressor locus 11p15, functions as an imprinting gene and exhibits suppressed expression across various malignant tumors. PHLDA2 plays a pivotal role in modulating the AKT signaling cascade in pulmonary malignancies,

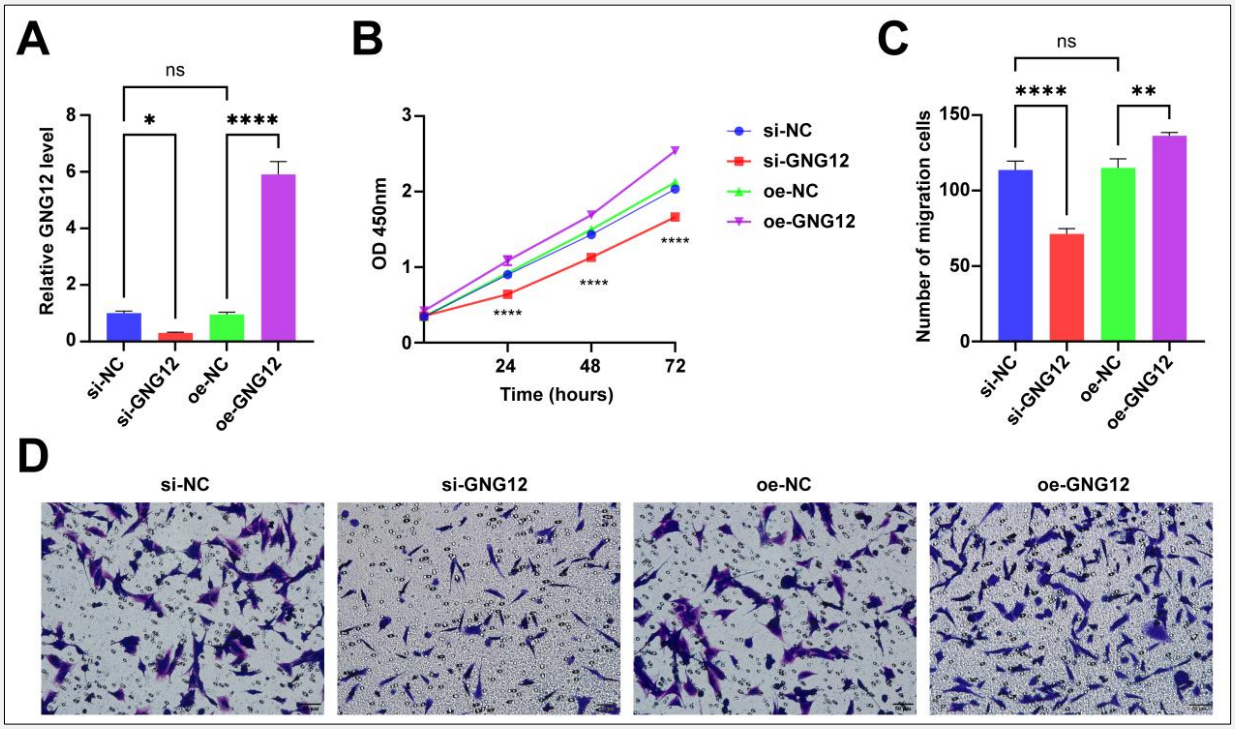

Figure 7. Effect of downregulating the expression of GNG12 on the proliferation and migration of neuroblastoma cells.

A - Detection of gene expression in neuroblastoma cells transfected with si-NC, si-GNG12, oe-NC, oe-GNG12, B - comparison of the effects of GNG12 downregulation on cell proliferation using the CCK-8 assay, C - results of the statistical analysis of the transwell cell migration assay, D - Transwell cell migration assay using SH-SY5Y cell line, comparing the number of migrated cells in si-NC group and si-GNG12 group, oe-NC group and oe-GNG12 group (magnification: *200) (** - p < 0.0001, *** - p < 0.001, ** - p < 0.01, * - p < 0.05).**

where it functions as a downstream target of oncogenic EGFR/ErbB2 signaling and inhibits cell proliferation by repressing AKT activation through a negative feedback loop [18]. In glioma models, elevated PHLDA2 expression attenuates cellular viability and proliferative capacity through negative regulation of the AKT/mTOR signaling axis, consequently promoting both apoptotic cell death and autophagic flux [19]. PHLDA2 also mediates ferroptosis, with its depletion suppressing reactive oxygen species (ROS)-induced ferroptosis, consequently facilitating tumor progression [20]. Furthermore, PHLD A2 demonstrates oncogenic activity through distinct molecular mechanisms in gastric [21] and hepatocellular malignancies [22]. Hence, PHLDA2 may participate in neuroblastoma by influencing either the AKT pathway or the biological functions of tumor cells.

GNG12, a gene encoding the G-gamma-12 protein belonging to the heterotrimeric G protein G12 subfamily, plays a key role in the regulation of tight junctions in endothelial cells [23]. Heterotrimeric G proteins, including GNG12, have been linked to the expression and distribution of tight junctions which form the blood-brain barrier [24,25]. Specifically, G-gamma-12 is known to interact with activated adrenergic receptors in central synapses [26]. Adrenergic receptors are involved in regulating protein kinase A (PKA) and cAMP levels, both of which affect the blood-brain barrier permeability [27]. Lower PKA levels lead to the opening of the blood-brain barrier, potentially facilitating the passage of leukemia cells into the central nervous system. Experimental evidence has demonstrated that targeted suppression of GNG12 expression significantly attenuates neoplastic cell proliferation and invasive potential, indicating its crucial role in modulating tumor initiation and progression across multiple malignancies, including glioblastoma and pancreatic adenocarcinoma [28]. In osteosarcoma, reduced GNG12 expression demonstrates significant correlation with adverse clinical outcomes, suggesting its utility as a prognostic molecular signature and its function as a critical modulator of disease progression [29]. Functionally, GNG12 is involved in regulating cell growth and casein synthesis through leucine-

mediated mTORC1 signaling, implying its impact on cancer pathology and potential as a prognostic biomarker for neuroblastoma [30].

Collagen-containing extracellular matrix (ECM) plays a pivotal role in tumors. Increased density and stiffness of ECM effectively promote tumor cell proliferation and survival. During tumor invasion and metastasis, the degradation and remodeling of collagen are crucial. Tumor cells degrade surrounding collagen by secreting specific enzymes, thereby creating favorable conditions for their migration. Moreover, ECM remodeling contributes to tumor angiogenesis by regulating the release and activity of cytokines, thus affecting vascular formation. ECM also affects immune evasion in tumors, either through physical barriers or by regulating the expression and activity of immune-modulatory molecules. In neuroblastoma, the enrichment of four biomarkers suggests that these genes may further influence the interaction between tumor cells and ECM by regulating the composition and function of the surrounding matrix. This interaction alters cell migration ability and invasiveness, thereby promoting tumor metastasis and dissemination [31].

DNA replication templated on existing DNA strands is essential for accurate transmission of genetic information. In tumors, the normal regulation of DNA replication is often disrupted. Perturbations in DNA replication fidelity and replication fork progression can precipitate genomic instability, potentially culminating in oncogene activation and tumor suppressor gene silencing, thereby promoting malignant transformation. Tumor cells typically experience high replication stress, further promoting genomic instability. Changes in the tumor microenvironment allow tumor cells to rapidly acquire new adaptive characteristics through genetic variation and selection, aiding their survival and spread [32].

Maintenance of chromosome regions is crucial for accurate transmission of genetic information. Epigenetic regulation alters gene expression patterns, affecting tumor cell behavior. Chromosomal instability not only changes gene expression and function but may also lead to further genetic heterogeneity, making tumors more adaptive and resistant to treatment. Regulation of the tumor microenvironment can influence the interaction between tumor cells and the surrounding environment, further affecting tumor growth and metastasis [33]. Changes in chromosome structure or function may affect tumor cell genetic stability and adaptability [34]. FBXO32 and GNG12 are enriched in DNA replication pathways and nuclear transport pathways. In neuroblastoma, upregulation of FBXO32 expression may promote faster cell cycle progression, accelerating DNA replication and aiding rapid proliferation of tumor cells. FBXO32 may ubiquitinate certain key nuclear transport proteins, affecting their degradation or activity. This regulation can alter the transport of proteins from the cytoplasm to the nucleus or vice versa, thereby affecting nuclear factor expression regulation and cellular responses. Activation or upregulation of GNG12 in neuroblastoma may support rapid cell division and growth of tumor cells by promoting growth signals or by regulating cellular responses. Its role in nuclear transport may involve regulating secondary messenger systems such as cAMP or calcium signaling, which can affect the activity and nuclear entry of key transcriptional activator proteins, thus influencing gene expression and cell behavior [35].

The enrichment of PHLDA2 and GRIA2 may suggest a role for these genes in regulating the interaction between tumor cells and the immune system, promoting immune escape. PHLDA2 enrichment may be related to its role in regulating cell responses to viral infections or viral-like stimuli. The extension of GRIA2 to regulate interactions with viral proteins and cytokines may be involved in regulating intracellular signaling pathways triggered by viral infections, affecting cellular response mechanisms such as apoptosis, proliferation, or inflammatory responses. The enrichment of these proteins may reflect their roles in regulating signaling pathways mediated by viral proteins or virus-like factors, affecting cell survival, proliferation, or inflammatory responses [36].

CONCLUSION

This comprehensive analysis identified four novel prognostic biomarkers in neuroblastoma (GRIA2, FBXO32, GNG12, and PHLDA2), with functional studies demonstrating that GNG12 depletion significantly attenuates neuroblastoma cell proliferation and migration, while its ectopic expression enhances these malignant phenotypes. These molecular insights advance our understanding of neuroblastoma pathogenesis and establish a foundation for improved prognostic stratification. The identification of these biomarkers not only reveals potential therapeutic targets but also provides opportunities for precision medicine approaches. Further mechanistic investigations into their regulatory networks may facilitate the development of targeted therapeutic interventions, potentially enhancing treatment efficacy through more precise patient stratification.

Acknowledgment:
The authors are grateful for the financial support that was provided for this study.

Ethical Approval and Consent to Participate:
The study only involved cell biology experiments; no human subject research or animal experiments were conducted. Therefore, ethical approval and consent to participate were not applicable. Clinical trial number: not applicable.

Availability of Data and Material:
All datasets utilized in the study are publicly available. The data analysis intermediate files are available from the corresponding author upon reasonable request.

Source of Funds:
This research was supported by the Guizhou Science and Technology Department 2023 (Qian ke he Foundation-ZK [2023] General 368) and the National Natural Science Foundation Cultivation Project of Guizhou Medical University (project no. 20NSP036).

Declaration of Interest:
The authors have no conflicts of interest to declare.

References:

1. Hanahan D, Weinberg RA. Hallmarks of cancer: the next generation. Cell 2011;144(5):646-74. (PMID: 21376230)

2. Baylin SB, Jones PA. A decade of exploring the cancer epigenome - biological and translational implications. Nat Rev Cancer 2011;11(10):726-34. (PMID: 21941284)

3. Henrich K-O, Bender S, Saadati M, et al. Integrative Genome-Scale Analysis Identifies Epigenetic Mechanisms of Transcriptional Deregulation in Unfavorable Neuroblastomas. Cancer Res 2016;76(18):5523-37. (PMID: 27635046)

4. Maggio V, Chierici M, Jurman G, Furlanello C. Distillation of the clinical algorithm improves prognosis by multi-task deep learning in high-risk Neuroblastoma. PLoS One 2018;13(12):e0208924. (PMID: 30532223)

5. Strother DR, London WB, Schmidt ML, et al. Outcome after surgery alone or with restricted use of chemotherapy for patients with low-risk neuroblastoma: results of Children's Oncology Group study P9641. J Clin Oncol 2012;30(15):1842-8. (PMID: 22529259)

6. Iommarini L, Ghelli A, Gasparre G, Porcelli AM. Mitochondrial metabolism and energy sensing in tumor progression. Biochim Biophys Acta Bioenerg 2017;1858(8):582-90. (PMID: 28213331)

7. Sakowicz-Burkiewicz M, Pawełczyk T, Zyśk M. Role of Energy Metabolism in the Progression of Neuroblastoma. Int J Mol Sci 2021;22(21):11421. (PMID: 34768850)

8. Konen LM, Wright AL, Royle GA, et al. A new mouse line with reduced GluA2 Q/R site RNA editing exhibits loss of dendritic spines, hippocampal CA1-neuron loss, learning and memory impairments and NMDA receptor-independent seizure vulnerability. Mol Brain 2020;13(1):27. (PMID: 32102661)

9. Zhang H-Y, Yang W, Lu J-B. Knockdown of GluA2 induces apoptosis in non-small-cell lung cancer A549 cells through the p53 signaling pathway. Oncol Lett 2017;14(1):1005-10. (PMID: 28693266)

10. Nakagawa T, Cheng Y, Ramm E, Sheng M, Walz T. Structure and different conformational states of native AMPA receptor complexes. Nature 2005;433(7025):545-9. (PMID: 15690046)

11. Ni T, Huang T, Gu S-L, et al. DRG Neurons Promote Perineural Invasion of Endometrial Cancer via GluR2. J Cancer 2020;11(9): 2518-28. (PMID: 32201522)

12. Zhou M, Qi L, Gu Y. GRIA2/ENPP3 Regulates the Proliferation and Migration of Vascular Smooth Muscle Cells in the Restenosis Process Post-PTA in Lower Extremity Arteries. Front Physiol 2021;12:712400. (PMID: 34504438)

13. Coombs ID, Ziobro J, Krotov V, Surtees T-L, Cull-Candy SG, Farrant M. A gain-of-function GRIA2 variant associated with neurodevelopmental delay and seizures: Functional characterization and targeted treatment. Epilepsia 2022;63(12):e156-63. (PMID: 36161652)

14. Vivero M, Doyle LA, Fletcher CDM, Mertens F, Hornick JL. GRIA2 is a novel diagnostic marker for solitary fibrous tumour identified through gene expression profiling. Histopathology 2014;65(1):71-80. (PMID: 24456377)

15. Zhou H, Liu Y, Zhu R, et al. FBXO32 suppresses breast cancer tumorigenesis through targeting KLF4 to proteasomal degradation. Oncogene 2017;36(23):3312-21. (PMID: 28068319)

16. Shu Y, Zhang H, Li J, Shan Y. LINC00494 Promotes Ovarian Cancer Development and Progression by Modulating NFκB1 and FBXO32. Front Oncol 2020;10:541410. (PMID: 33585183)

17. Liao X, Li Z, Zheng H, et al. Downregulation of BASP1 Promotes Temozolomide Resistance in Gliomas via Epigenetic Activation of the FBXO32/NF-κB/MGMT Axis. Mol Cancer Res 2023;21(7):648-63. (PMID: 36961398)

18. Wang X, Li G, Koul S, et al. PHLDA2 is a key oncogene-induced negative feedback inhibitor of EGFR/ErbB2 signaling via interference with AKT signaling. Oncotarget 2018;9(38):24914-26. (PMID: 29861842)

19. Guo C, Liu S, Zhang T, Yang J, Liang Z, Lu S. Knockdown of PHLDA2 promotes apoptosis and autophagy of glioma cells through the AKT/mTOR pathway. J Neurogenet 2022;36(2-3): 74-80. (PMID: 35894264)

20. Yang X, Wang Z, Samovich SN, et al. PHLDA2-mediated phosphatidic acid peroxidation triggers a distinct ferroptotic response during tumor suppression. Cell Metab 2024;36(4):762-77.e9. (PMID: 38309267)

21. Koh SA, Lee KH. HGF-mediated Up-regulation of PHLDA2 Is Associated With Apoptosis in Gastric Cancer. Anticancer Res 2021;41(9):4377-85. (PMID: 34475057)

22. Wang S, Wang Y-F, Yang G, et al. Heat shock protein family A member 8 serving as a co-activator of transcriptional factor ETV4 up-regulates PHLDA2 to promote the growth of liver cancer. Acta Pharmacol Sin 2023;44(12):2525-36. (PMID: 37474643)

23. Li J, Jin C, Zou C, et al. GNG12 regulates PD-L1 expression by activating NF-κB signaling in pancreatic ductal adenocarcinoma. FEBS Open Bio 2020;10(2):278-87. (PMID: 31898405)

24. Langen UH, Ayloo S, Gu C. Development and Cell Biology of the Blood-Brain Barrier. Annu Rev Cell Dev Biol 2019;35:591-613. (PMID: 31299172)

25. González-Mariscal L, Raya-Sandino A, González-González L, Hernández-Guzmán C. Relationship between G proteins coupled receptors and tight junctions. Tissue Barriers 2018;6(1): e1414015. (PMID: 29420165)

26. Yim YY, Betke KM, McDonald WH, et al. The *in vivo* specificity of synaptic Gβ and Gγ subunits to the α(2a) adrenergic receptor at CNS synapses. Sci Rep 2019;9(1):1718. (PMID: 30737458)

27. Shi Q, Li M, Mika D, et al. Heterologous desensitization of cardiac β-adrenergic signal via hormone-induced βAR/arrestin/PDE4 complexes. Cardiovasc Res 2017;113(6):656-70. (PMID: 28339772)

28. Guzman-Martinez L, Calfío C, Farias GA, Vilches C, Prieto R, Maccioni RB. New Frontiers in the Prevention, Diagnosis, and Treatment of Alzheimer's Disease. J Alzheimers Dis 2021;82(s1): S51-63. (PMID: 33523002)

29. Yuan J, Yuan Z, Ye A, et al. Low GNG12 Expression Predicts Adverse Outcomes: A Potential Therapeutic Target for Osteosarcoma. Front Immunol 2021;12:758845. (PMID: 34691083)

30. Luo C, Zhao S, Dai W, Zheng N, Wang J. Proteomic analyses reveal GNG12 regulates cell growth and casein synthesis by activating the Leu-mediated mTORC1 signaling pathway. Biochim Biophys Acta Proteins Proteom 2018;1866(11):1092-101. (PMID: 30282607)

31. Cescon M, Rampazzo E, Bresolin S, et al. Collagen VI sustains cell stemness and chemotherapy resistance in glioblastoma. Cell Mol Life Sci 2023;80(8):233. (PMID: 37505240)

32. Li H, Zimmerman SE, Weyemi U. Genomic instability and metabolism in cancer. Int Rev Cell Mol Biol 2021;364:241-65. (PMID: 34507785)

33. Koboldt DC, Zhang Q, Larson DE, et al. VarScan 2: somatic mutation and copy number alteration discovery in cancer by exome sequencing. Genome Res 2012;22(3):568-76. (PMID: 22300766)

34. Li J, Duran MA, Dhanota N, et al. Metastasis and Immune Evasion from Extracellular cGAMP Hydrolysis. Cancer Discov 2021; 11(5):1212-27. (PMID: 33372007)

35. Li L, Sun B, Sun Y. Identification of functional TF-miRNA-hub gene regulatory network associated with ovarian endometriosis. Front Genet 2022;13:998417. (PMID: 36212136)

36. Wang Y, Huang J, Zhang J, Wang F, Tang X. Identifying biomarkers associated with the diagnosis of ulcerative colitis via bioinformatics and machine learning. Math Biosci Eng 2023;20(6): 10741-56. (PMID: 37322958)

Additional material can be found online at:
http://supplementary.clin-lab-publications.com/250323/